

Effects of spin-orbit interaction on the magnetic and electronic structure of antiferromagnetic LaFeAsO

Jung-Hoon Lee,¹ Hyun Myung Jang,^{1,2} and Hyoung Joon Choi^{3,*}

¹*Department of Materials Science and Engineering, and Division of Advanced Materials Science, Pohang University of Science and Technology (POSTECH), Pohang 790-784, Republic of Korea*

²*Department of Physics, Pohang University of Science and Technology (POSTECH), Pohang 790-784, Republic of Korea*

³*Department of Physics and IPAP, Yonsei University, Seoul 120-749, Republic of Korea*

(Dated: December 30, 2018)

Magnetic and electronic structures in LaFeAsO in the single-stripe-type antiferromagnetic (AFM) phase are studied using first-principles density-functional calculations including the spin-orbit interaction. We find that the longitudinal ordering (LO) where Fe magnetic moments are parallel or anti-parallel with the in-plane AFM ordering vector, \mathbf{q} , is lower in energy than transverse orderings (TOs) where Fe magnetic moments are perpendicular to \mathbf{q} , in excellent agreement with recent neutron diffraction experiments. Calculated energy difference between LO and TOs is about 0.2 meV per Fe atom, indicating that LO will prevail at temperature below 2 K. We also find that the spin-orbit interaction splits degenerate bands at $\mathbf{k} = (1/2)\mathbf{q}$ by about 60 meV, depending on spatial directions of the Fe magnetic moments.

PACS numbers: 74.70.Xa, 71.15.Mb, 75.70.Tj, 71.70.Ej

Superconductivity and magnetism in iron oxypnictides LaFeAsO and other $R\text{FeAsO}$ (R = rare-earth) have become central issues since their discovery.¹⁻³ These materials exhibit superconductivity at high temperatures, for example, 55 K in $\text{SmFeAsO}_{1-x}\text{F}_x$.⁴ Without doping, these compounds show antiferromagnetism at low temperature, and they become superconductors when doped with electrons or holes. The occurrence of superconductivity in the vicinity of magnetic phase suggests that understanding the magnetic properties could be essential in revealing the origin of their unconventional superconductivity.⁵⁻¹⁴

As temperature lowers, undoped LaFeAsO undergoes a structural transition from a tetragonal to an orthorhombic structure and Fe magnetic moments form a single-stripe-type antiferromagnetic (AFM) ordering, where Fe magnetic moments are ordered antiferromagnetically in an orthorhombic in-plane axis, say a -axis, ferromagnetically in the other in-plane axis, say b -axis, and antiferromagnetically along the c -axis.⁶ Density functional calculations have been successful in predicting and explaining the in-plane AFM orderings of Fe magnetic moments in iron pnictides^{5,7,8,10,12,15,16} and chalcogenides^{17,18} correctly although the calculations predict substantially large values of Fe magnetic moments.

More recently, neutron diffraction experiments¹⁹ on the magnetic structure in LaFeAsO claimed that spatial directions of Fe magnetic moments in the single-stripe-type AFM phase are collinear with the AFM direction in the Fe plane, i.e., the orthorhombic a -axis, rather than other directions.¹⁹ This result suggests a significant role of the spin-orbit interaction in LaFeAsO, since magnetic moments are coupled to the lattice structure via the spin-orbit interaction only; yet, there is no theoretical report on this issue.

In this Communication, we will present electronic and magnetic properties in LaFeAsO calculated by first-

principles density-functional methods including the spin-orbit interaction. We will show that spatial directions of Fe magnetic moments in the ground state of the single-stripe-type AFM are along the in-plane AFM direction, i.e., the orthorhombic a -axis, which is consistent with the recent neutron diffraction experiments.¹⁹ We will also show that the energy cost for aligning Fe magnetic moments perpendicular to the orthorhombic a -axis is about 0.2 meV/Fe, indicating that the Fe magnetic moments prefer the orthorhombic a -axis direction significantly at temperatures below 2 K. In addition, we show that the spin-orbit interaction splits degenerate bands at a high-symmetry point, X, in the orthorhombic Brillouin zone by about 60 meV, depending on spatial directions of the Fe magnetic moments.

Our first-principles calculations are performed with the generalized gradient approximation²⁰ to the density functional theory and the projector-augmented-wave pseudopotentials^{21,22} as implemented in VASP.^{23,24} We regard $4p^65s^26d^1$ electrons in La, $3p^63d^64s^2$ in Fe, $4s^24p^3$ in As, and $2s^22p^4$ in O as valence electrons. All of our calculations are performed using a $8 \times 8 \times 4$ Monkhorst-Pack k -point mesh²⁵ centered at Γ for orthorhombic ($Cmme$) structure. Electronic wavefunctions are expanded with plane waves up to a kinetic-energy cutoff of 500 eV, and the tetrahedron method with the Blöchl corrections is used for the Brillouin zone integration.²⁶ With the spin-orbit interaction included in the total-energy functional, we carefully check the convergence of the self-consistent calculation of the electron density in order to distinguish small difference in the total energy caused by difference in the spatial directions of the Fe magnetic moments.

We optimize atomic positions in LaFeAsO using a 32-atom orthorhombic supercell, $a \times b \times 2c$, which is twice the structure shown in Fig. 1(a) along the c -axis. During the optimization, the supercell lattice constants are fixed to $a = 5.7063$ Å, $b = 5.6788$ Å, and $c = 8.7094$ Å,

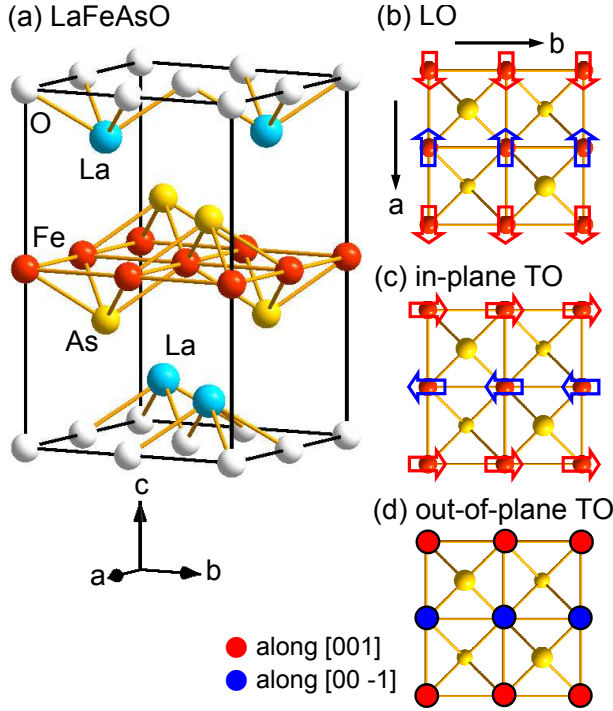


FIG. 1: (Color online) Atomic and magnetic structures in LaFeAsO. (a) An orthorhombic unit cell of LaFeAsO in the single-stripe-type antiferromagnetic phase. The unit cell contains four formula units, i.e., 16 atoms. (b) Longitudinal ordering (LO), (c) in-plane transverse ordering (TO), and (d) out-of-plane TO of Fe magnetic moments in the FeAs layer. In LO, in-plane TO, and out-of-plane TO, spatial directions of Fe magnetic moments are parallel or anti-parallel with the orthorhombic a , b , and c directions, respectively. In (b) and (c), directions of Fe magnetic moments are denoted by arrows. In (d), Fe magnetic moments in the upper and the lower rows (in red) are in the c direction, while those in the middle row (in blue) are in the opposite direction.

which are the measured values at 2 K,¹⁹ and the single-stripe-type AFM order is imposed, where Fe magnetic moments are antiferromagnetic along the a direction and ferromagnetic along the b direction. Atomic positions are fully optimized until residual forces on them are less than 0.005 eV/Å. The spin-orbit interaction is considered during the structural optimization, but obtained equilibrium positions of atoms depend negligibly on spatial directions of Fe magnetic moments as long as they are in the single-stripe-type AFM.

To investigate effects of the spin-orbit interaction on the Fe magnetic-moment directions, we consider three different configurations, as shown in Figs. 1(b)-(d), where the Fe magnetic moments are along the orthorhombic a , b , and c directions, respectively. In Fig. 1(b), the Fe magnetic moments are in a longitudinal order (LO) in the sense that they are parallel or anti-parallel to the in-plane AFM direction, i.e., the a -axis in our supercell. In Figs. 1(c) and (d), the Fe magnetic moments are in

TABLE I: Calculated total energies, E_{tot} , and Fe magnetic moments m_{Fe} , in LaFeAsO with various spin-configurations, obtained including the spin-orbit interaction. Considered spatial directions of Fe magnetic moments are the longitudinal ordering (LO), the in-plane transverse ordering (TO), and the out-of-plane TO, as shown in Fig. 1. For each spin configuration, we consider antiferromagnetic (AFM) and ferromagnetic (FM) orderings along the c axis; in the former Fe moment directions are in phase along the c axis, while in the latter they are out of phase along the c axis. The total energy of LO with AFM along the c -axis is set to zero. Without the spin-orbit interaction, all spin-configurations have the same total energy and the same Fe magnetic moment, 1.689 μ_{B}/Fe .

spin configuration		E_{tot} (meV/Fe)	m_{Fe} (μ_{B}/Fe)
AFM	LO	0.00	1.680
along c -axis	in-plane TO	0.25	1.682
	out-of-plane TO	0.15	1.681
FM	LO	0.00	1.680
along c -axis	in-plane TO	0.25	1.682
	out-of-plane TO	0.15	1.681

in-plane and out-of-plane transverse orders (TOs), respectively, in the sense that they are perpendicular to the in-plane AFM direction and they are either in the Fe plane or out of the plane. Although the spatial directions of Fe magnetic moments are different in the three configurations, all of them have the same single-stripe-type AFM in the sense that neighboring Fe magnetic moments are in opposite directions along the a direction while they are in the same direction along the b direction. For each of the three configurations, we consider two different inter-Fe-plane magnetic orderings: ferromagnetic and antiferromagnetic orderings between Fe magnetic moments neighboring along the c direction.

In our density-functional calculations, we do not impose any constraint on the spatial direction of the Fe magnetic moments; however, when we take one of the three configurations as initial guess for the spin density at the start of the self-consistent iteration in our calculations, the spatial directions of the Fe magnetic moments are stationary during the iteration until the self-consistency is reached. In the cases that we try spatial directions of Fe magnetic moments slightly away from the LO case as initial guess, the directions of the Fe magnetic moments are changed during the self-consistent iteration and they converge to the LO case.

Table I shows our calculational results for the total energy and Fe magnet moments of LaFeAsO including the spin-orbit interaction. We find that LO is the lowest-energy configuration, while in-plane TO and out-of-plane TO are higher in energy than LO by 0.25 meV and 0.15 meV per Fe atom, respectively. The total energies in our calculations are independent of c -axis orderings of Fe magnetic moments because of rather large distance between Fe planes in LaFeAsO. Obtained Fe magnetic mo-

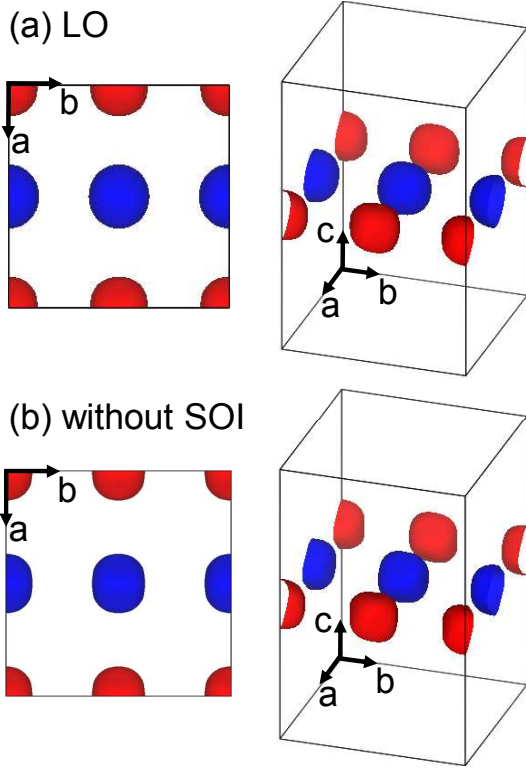


FIG. 2: (Color online) Calculated spin densities in LaFeAsO in the single-stripe-type AFM phase, represented with iso-surfaces. (a) The a -axis component of the spin density with the spin-orbit interaction in the case of the longitudinal ordering (LO) of Fe magnetic moments. (b) Spin density without the spin-orbit interaction, drawn for comparison. In (a) and (b), left panels show top views of the spin density in Fe planes in which Fe atoms are at corners, at middles of edges, and at the center of the square, and the right panels show corresponding three-dimensional views of the spin density in the orthorhombic unit cell. In each top view, iso-surfaces in the upper and lower rows (in red) correspond to a positive spin density while those in the middle row (in blue) correspond to a negative one.

ments are $1.680 \mu_B/\text{Fe}$ for LO, $1.682 \mu_B/\text{Fe}$ for in-plane TO, and $1.681 \mu_B/\text{Fe}$ for out-of-plane TO, which are also independent of c -axis orderings of Fe magnetic moments. Without the spin-orbit interaction, all the three configurations have the same total energy and the same Fe magnetic moment, $1.689 \mu_B/\text{Fe}$.

Our result that LO is the lowest-energy configuration of Fe magnetic moments in LaFeAsO is in excellent agreement with the recent neutron diffraction experiments¹⁹ where spatial directions of Fe magnetic moments at 2 K in LaFeAsO were claimed to be along the AFM direction in the Fe plane. The same neutron diffraction experiments report that the size of the Fe magnetic moment in LaFeAsO is $0.63 \mu_B/\text{Fe}$ at 2 K,¹⁹ so our calculated sizes of Fe magnetic moments are about one Bohr magneton larger than the measured value. Since our calculated energy gain of LO is about 0.2 meV/Fe when compared

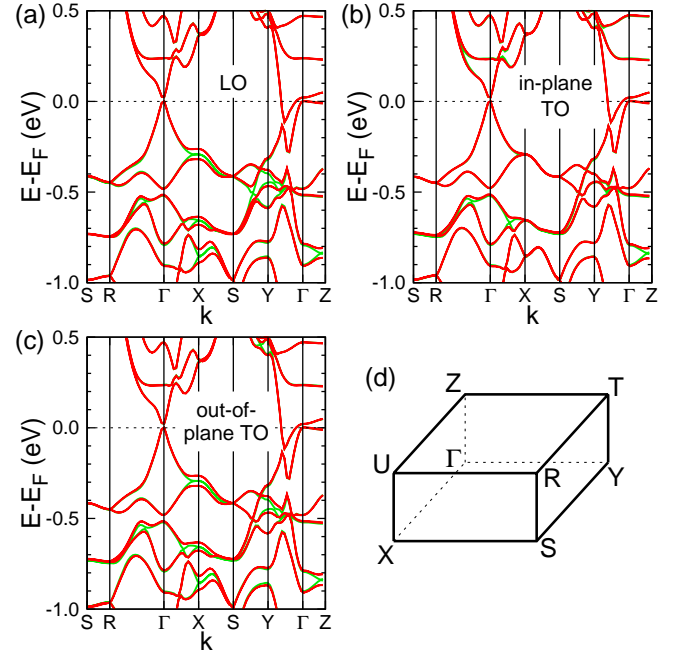


FIG. 3: (Color online) Electronic energy bands along the high symmetry lines in LaFeAsO for three different spin-configurations: (a) LO, (b) in-plane TO, and (c) out-of-plane TO. Dark gray (red) and light gray (green) lines represent results obtained with and without the spin-orbit interaction, respectively. (d) One eighth of the first Brillouin zone, where high symmetry points and lines are marked. In (a) and (c), splitting of degenerate bands at the X point by the spin-orbit interaction is about 60 meV. In (d), Γ -X, Γ -Y, and Γ -Z lines are along the orthorhombic a -, b -, and c -axis in Fig. 1, respectively.

with the other magnetic configurations and this energy gain corresponds to a temperature of about 2 K, our result implies that LO is thermodynamically preferred at temperatures below 2 K.

As shown in Table I, obtained magnitudes of Fe magnetic moments are very weakly dependent on the spatial directions of the moments, and the spin-orbit interaction produces only $0.008 \mu_B/\text{Fe}$ difference. For more detailed comparison, we obtain the spatial distributions of the spin densities in LaFeAsO with and without the spin-orbit interaction, as shown in Fig. 2, and find that the maximal difference in the spin densities in the two cases is about 10% of the maximal size of the spin density in each case. In Fig. 2, the spin densities with and without the spin-orbit interaction look quite similar to each other, but it can be seen more easily in the top views in Fig. 2 that the shapes of the iso-surfaces are slightly different.

We study effects of the spin-orbit interaction on the electronic band structures in LaFeAsO. Figure 3 shows the band structures in orthorhombic LaFeAsO, where dark gray (red) and light gray (green) lines show the band structures with and without the spin-orbit interaction, respectively. Since most of the band structures without the spin-orbit interaction coincide with those with the

spin-orbit interaction and the former is drawn prior to the latter, the band structures without the spin-orbit interaction, plotted in light gray (green), are visible only at k -points where the spin-orbit interaction produces significant difference. Band structures without the spin-orbit interaction are consistent with previous theoretical results.^{8,17} Our results show that the spin-orbit interaction splits degenerate bands at the X point in the LO case [Fig. 3(a)] and in the out-of-plane TO case [Fig. 3(c)], and the splitting is about 60 meV. However, band structures in the in-plane TO case [Fig. 3(b)] do not show significant splitting at the X point even with the spin-orbit interaction. This dependence of band-energy splitting on the spatial direction of Fe magnetic moments is due to specific orbital characters of the electronic states at the X point.

In summary, we have investigated the effects of the spin-orbit interaction in the magnetic- and electronic structures of the FeAs-based compound LaFeAsO using

first-principles density functional calculations. In our results, the longitudinal ordering of Fe magnetic moments, in which the moments are parallel or anti-parallel with the in-plane AFM direction, is the lowest-energy magnetic structure among various spin-configurations. This is in good agreement with the experimental results¹⁹ although the magnitude of our calculated magnetic moment is about one Bohr magneton larger than the experimental value. We also find that the energy gain of the directional alignment of Fe magnetic moments in LaFeAsO is about 0.2 meV/Fe, equivalent to a temperature of 2 K, and that the spin-orbit interaction splits degenerate bands at the X point by about 60 meV, depending on the spatial direction of the Fe magnetic moments.

This work was supported by National Research Foundation of Korea (Grant No. 2009-0081204). Computational resources have been provided by KISTI Supercomputing Center (Project No. KSC-2008-S02-0004).

-
- * Email: h.j.choi@yonsei.ac.kr
- ¹ Y. Kamihara, H. Hiramatsu, M. Hirano, R. Kawamura, H. Yanagi, T. Kamiya, and H. Hosono, *J. Am. Chem. Soc.* **128**, 10012 (2006).
 - ² Y. Kamihara, T. Watanabe, M. Hirano, and H. Hosono, *J. Am. Chem. Soc.* **130**, 3296 (2008).
 - ³ H. Takahashi, K. Igawa, K. Arii, Y. Kamihara, M. Hirano, and H. Hosono, *Nature (London)* **453**, 376 (2008).
 - ⁴ Z.-A. Ren, W. Lu, J. Yang, W. Yi, X.-L. Shen, Z.-C. Li, G.-C. Che, X.-L. Dong, L.-L. Sun, F. Zhou, and Z.-X. Zhao, *Chin. Phys. Lett.* **25**, 2215 (2008).
 - ⁵ I. I. Mazin, D. J. Singh, M. D. Johannes, and M. H. Du, *Phys. Rev. Lett.* **101**, 057003 (2008).
 - ⁶ C. de la Cruz, Q. Huang, J. W. Lynn, J. Li, W. R. II, J. L. Zarestky, H. A. Mook, G. F. Chen, J. L. Luo, N. L. Wang, and P. Dai, *Nature (London)* **453**, 899 (2008).
 - ⁷ T. Yildirim, *Phys. Rev. Lett.* **101**, 057010 (2008).
 - ⁸ Z. P. Yin, S. Lebegue, M. J. Han, B. P. Neal, S. Y. Savrasov, and W. E. Pickett, *Phys. Rev. Lett.* **101**, 047001 (2008).
 - ⁹ H.-H. Klauss, H. Luetkens, R. Klingeler, C. Hess, F. J. Litterst, M. Kraken, M. M. Korshunov, I. Eremin, S. -L. Drechsler, R. Khasanov, A. Amato, J. Hamann-Borrero, N. Leps, A. Kondrat, G. Behr, J. Werner, and B. Buchner, *Phys. Rev. Lett.* **101**, 077005 (2008).
 - ¹⁰ J. Dong, H. J. Zhang, G. Xu, Z. Li, G. Li, W. Z. Hu, D. Wu, G. F. Chen, X. Dai, J. L. Luo, Z. Fang, and N. L. Wang, *Europhys. Lett.* **83**, 27006 (2008).
 - ¹¹ B. Lorenz, K. Sasmal, R. P. Chaudhury, X. H. Chen, R. H. Liu, T. Wu, and C. W. Chu, *Phys. Rev. B* **78**, 012505 (2008).
 - ¹² I. I. Mazin, M. D. Johannes, L. Boeri, K. Koepernik, and D. J. Singh, *Phys. Rev. B* **78**, 085104 (2008).
 - ¹³ W. Z. Hu, J. Dong, G. Li, Z. Li, P. Zheng, G. F. Chen, J. L. Luo, and N. L. Wang, *Phys. Rev. Lett.* **101**, 257005 (2008).
 - ¹⁴ V. Cvetkovic and Z. Tesanovic, *Europhys. Lett.* **85**, 37002 (2009).
 - ¹⁵ C.-Y. Moon, S. Y. Park, and H. J. Choi, *Phys. Rev. B* **78**, 212507 (2008).
 - ¹⁶ C.-Y. Moon, S. Y. Park, and H. J. Choi, *Phys. Rev. B* **80**, 054522 (2009).
 - ¹⁷ F. Ma, W. Ji, J. Hu, Z.-Y. Lu, and T. Xiang, *Phys. Rev. Lett.* **102**, 177003 (2009).
 - ¹⁸ C.-Y. Moon and H. J. Choi, *Phys. Rev. Lett.* **104**, 057003 (2010).
 - ¹⁹ N. Qureshi, Y. Drees, J. Werner, S. Wurmehl, C. Hess, R. Klingeler, B. Büchner, M. T. Fernández-Díaz, and M. Braden, arXiv:1002.4326.
 - ²⁰ J. P. Perdew, K. Burke, and Y. Wang, *Phys. Rev. B* **54**, 16533 (1996).
 - ²¹ P. E. Blöchl, *Phys. Rev. B* **50**, 17953 (1994).
 - ²² G. Kresse and D. Joubert, *Phys. Rev. B* **59**, 1758 (1999).
 - ²³ G. Kresse and J. Hafner, *Phys. Rev. B* **47**, 558(R) (1993).
 - ²⁴ G. Kresse and J. Furthmüller, *Phys. Rev. B* **54**, 11169 (1996).
 - ²⁵ H. J. Monkhorst and J. D. Pack, *Phys. Rev. B* **13**, 5188 (1976).
 - ²⁶ P. E. Blöchl, O. Jepsen, and O. K. Andersen, *Phys. Rev. B* **49**, 16223 (1994).
 - ²⁷ Y. Yang and X. Hu, *J. Appl. Phys.* **106**, 073910 (2009).